Proceedings of the 12th International Coral Reef Symposium, Cairns, Australia, 9-13 July 2012
1A Reefs Through Time

Assessing reef island response to environmental conditions on the GBR

Sarah Hamylton[1], Marji Puotinen[1, 2]

[1]School of Earth and Environmental Sciences, University of Wollongong, Wollongong, NSW 2505, Australia
[2]School of Earth Sciences, The Ohio State University, Columbus, Ohio 43210, USA
Corresponding author: shamylto@uow.edu.au

Abstract. Reef island cays form through the deposition of sediment as a result of wave trains converging across reef platforms and, at the regional scale, are influenced by a range of oceanographic and physical environmental factors. Preliminary results of a spatial modeling exercise applied to 103 reef islands are presented, demonstrating that variation in island area and volume can be accurately expressed as a function of latitudinal and cross-shelf gradients in regional oceanographic factors (exposure to incident waves, tidal range and the frequency of tropical cyclones) and local physical factors (position on the shelf, area of supporting reef platform, area of vegetative cover). This morphometric autoregressive model reveals important differences in the response of unvegetated cays, vegetated cays and low wooded islands to their local environmental conditions. The empirical relationships defined could further be used to simulate future island accretionary and erosional dynamics, and consequent vulnerability given information on anticipated environmental changes.

Key words: Cay, Accretion, Erosion, Cyclone, Wave energy.

Introduction

Reef cays develop through contemporary geomorphological processes that deposit sediments at convergence points where opposing wave trains have been refracted in a centripetal fashion around reef platforms (Smithers and Hopley, 2011). After substantial deposition, cays may undergo a developmental progression from unvegetated to "mature", fully developed, low wooded islands (Fairbridge and Teichert, 1948). Under optimal conditions and through the interplay of processes across multiple spatial and temporal scales, a reef island will grow in size until an equilibrium is reached whereby sediment delivery and removal are balanced (Hopley et al., 2007; Stoddart and Steers, 1977).

The Great Barrier Reef (GBR) spans a latitudinal range of 15 degrees and, including the Torres Strait, supports over 1100 islands extending from the mainland to the shelf edge. The different island types evident (unvegetated cays, vegetated cays, low wooded islands) have formed under varying local contemporary environmental conditions such as exposure to incident waves, tidal range and the frequency of tropical cyclones that have given rise to distinct geographical patterns in both island characteristics (Hopley et al., 1989) and cay mobility (Aston, 1995).

This paper presents the preliminary results of a morphometric geostatistical analysis of 103 reef islands on the GBR (13 unvegetated cays, 43 vegetated cays and 47 low wooded islands, see Fig. 1). Two key characteristics of reef islands, their area and volume, are modelled as an autoregressive function of their environmental settings. Environmental settings are characterised through corresponding datasets that quantify both regional oceanographic factors (exposure to incident waves, tidal range and the frequency of tropical cyclones) and local physical factors (position on the shelf, area of supporting reef platform, area of vegetative cover) influencing reef islands.

Material and Methods

Characterising island properties: Area and volume

The study employed an independently validated subset of the Great Barrier Reef Marine Park Authority's "GBR Features" dataset, which, in terms of detail, is among the best available that extends across the whole GBR. Spatially referenced vector datasets representing each of the 103 islands selected for the study and their associated reef platform were exported and their configuration was independently verified against a Landsat TM satellite image mosaic of the GBR made up of 11 images acquired between 2003 and 2005. Verification proceeded by overlaying the vector dataset onto the satellite image and visually inspecting the correspondence of the island and reef platform outline with that apparent on the satellite

image at a scale of 1:1000. Where an offset was apparent, the vector dataset was edited to coincide with the landform boundary apparent on the satellite image.

The area of each island was calculated using ArcGIS and the volume of the islands was calculated by overlaying the vector dataset onto a digital elevation model (resolution 100 m, accuracy <2 m) that depicted island height (Beaman, 2010) and calculating the total elevation of digital elevation model (DEM) pixels falling within each island boundary.

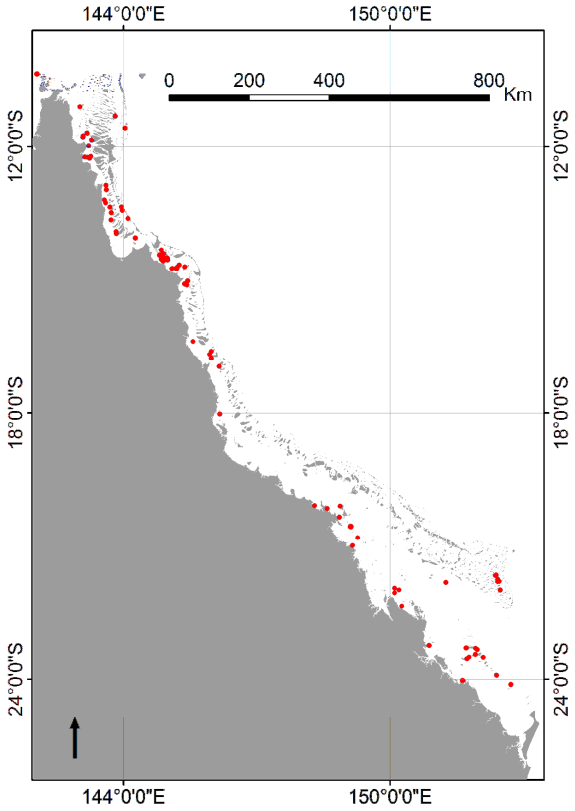

Figure 1: Location of the 103 islands selected for the morphometric assessment (denoted as red dots).

Characterising local environmental setting

Tidal range

Data from the nine tide gauges comprising the National Tidal Centre's Queensland tidal gauge network were acquired for the period 1995 to 2005 and highest astronomical tide was extracted from each gauge dataset. These values were then plotted in their locations and a spatial interpolation was performed to generate a continuous surface representing maximum tidal range across the study area (Fig. 2).

Incident wave energy

For each island setting, a fetch-based analysis was used to estimate relative exposure to typical incident wind-driven wave energy (Pepper and Puotinen, 2009; Hill et al., 2010). Fetch was calculated at 1 km intervals around reef platform boundaries and potential wave blocking obstacles were defined as land, island and reef. Wind data were input from 8 weather stations around the GBR for the time period 1999- 2005 and each site was assigned to the nearest weather station using a voronnoi tessellation (Longley et al., 2010). The maximum possible fetch line was defined on the basis of the maximum non-cyclonic wind speed measured at each station (Pepper and Puotinen, 2009). Radial lines of this maximum distance were generated at 7.5° intervals around each measurement site and fetch was calculated as the distance to the nearest wave blocking obstacle in each direction. Each distance within a given site's array of fetch lines was then weighted based on the % frequency of wind for a given direction under typical conditions and normalized into a dimensionless number that represented relative wave exposure (RWE), ranging from 0 (sheltered) to 1 (completely exposed). A range of metrics were derived from the relative wave exposure measurements around the reef platform perimeter (sum and average RWE around the complete reef platform perimeter, sum and average RWE around the exposed and sheltered portions of the reef platform perimeter) and tested for correspondence with island characteristics. Of these, the average exposed relative wave energy had the greatest individual correspondence with island characteristics and this was therefore selected for use in the autoregressive modeling.

Tropical cyclone frequency

Exposure to tropical cyclone conditions was modeled for the period 1985 – 2005 to align with the island datasets. While this represents a short time series given the temporal scales of natural variability in cyclone behavior, representing the spread of cyclone gale winds before 1985 is problematic due to poor data quality (Landsea et al., 2006). A spatially continuous tropical cyclone raster model was developed which defined cyclone activity as the number of days per year that a component pixel was exposed to winds of at least gale force (17 ms^{-1}). This was based on analysis of historical tropical cyclone track data for each cyclone season (November to May) from the International Best Track Archive for Climate Stewardship (IBTRACS) Tropical Cyclone dataset using techniques reported in Carrigan and Puotinen (2011).

Cross-shelf location

For each of the 103 selected islands, the Euclidean distance between the centroid of the polygon depicting the island and the Queensland coastline, as was calculated as a measure of cross-shelf location. In this way, the distance across the shelf was expressed as a continuous variable and incorporated the varying width of the shelf itself with latitude.

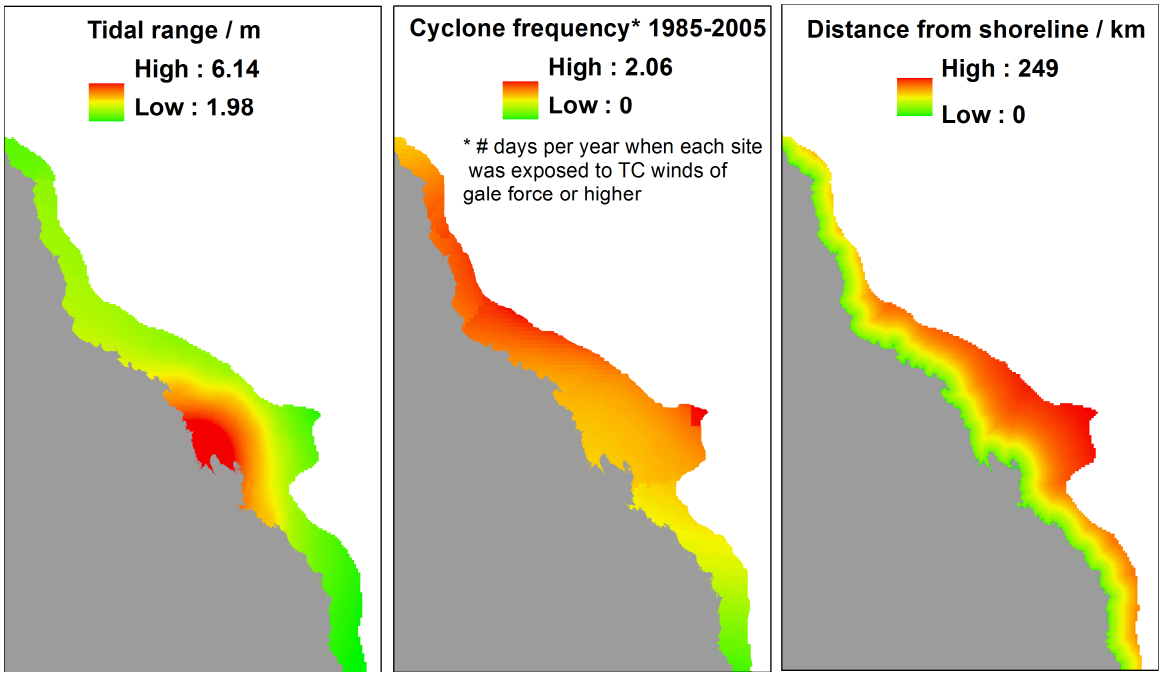

Figure 2 Spatial distribution of the environmental conditions (explanatory variables) used as input to the autoregressive model. Only spatially continuous input variables are shown.

Reef platform area

Reef platform areas were calculated from the validated GBRMPA dataset. The area of the spatially referenced polygons representing each of the 103 reef platforms supporting the islands was calculated using ArcGIS.

Vegetative area

The area of each study island covered by vegetation was digitised from the Landsat mosaic of the study islands at a scale of 1:1000 and the vegetative area was expressed as the percentage of the island area that was covered by vegetation.

Development of an autoregressive model of reef island area and volume

Two autoregressive equations were applied to model the area and volume (dependent variables) of each island as a function of the local environmental conditions captured by the explanatory variables. A spatially explicit autoregressive component was included in the equation to avoid violating the assumption of independence of observations and incorporate any spatial autocorrelation in the nature of reef island character by drawing explicitly on the location of each individual island through the construction of a spatial weights matrix (w(i,j)) that expressed for each island in the dataset whether or not other islands belonged to its neighbourhood, such that wij=1 when islands i and j were neighbours and wij=0 otherwise (Anselin and Bera, 1998). In this way, the values of the dependent variable at neighbouring locations were utilised in the model specification:

$$\mu_{(i)} = \beta_0 + \beta_1 X_{1(i)} + \beta_2 X_{2(i)} + \ldots + \beta_k X_{k(i)} + \rho \sum_{j \in N(i)} w(i,j) Y(j) + e_{(i)} \quad i = 1, \ldots, 130 \qquad \text{Eqn 2}$$

where $X_1 - X_6$ are the six explanatory variables, e(i) = independent, normally distributed error term β_0 to β_6 = coefficients estimated using the model and ρ = a parameter associated with the interaction effect.

For each island, a model building approach was applied that iteratively went through every possible combination of independent variables and tested the performance of these in explaining the observed variation in island area and volume. The diagnostics associated with the results of the highest performing models (for low wooded islands, vegetated cays and unvegetated cays) were reported.

Results

For unvegetated cays the best performing model related to island area, while for vegetated cays and low wooded islands, the best performing models related to island volume. All of the explanatory variables were significant at a level of $p = 0.08$, with many below $p = 0.001$ (Table 1).

For the unvegetated cays model, the explanatory variable with the highest z-score was distance to mainland, while for the vegetated cays this was cyclone frequency and for the low wooded islands this was reef area.

Unvegetated cays (*island area*) R^2		**0.89**
Variable	**Z-score (p value)**	**ε**
Distance to mainland	-2.41 (<0.02)	0.00
Tidal range	1.28 (<0.001)	0.00
Cyclone frequency	1.15 (<0.02)	0.00
Average exposed RWE	1.47 (<0.01)	0.01
Reef Area	0.37 (0.1)	0.00
Vegetated cays *(island volume)* R^2		**0.73**
Variable	**Z-score (p value)**	**ε**
Distance to mainland	-1.97 (p<0.01)	3.23
Tidal range	60.70 (p<0.001)	0.42
Cyclone frequency	-64.10 (p<0.001)	0.49
Average exposed RWE	62.20 (p<0.001)	4.51
% Vegetative cover	43.34 (p<0.001)	0.01
Reef Area	45.03 (p<0.001)	0.00
Low wooded islands *(island volume)* R^2		**0.79**
Variable	**Z-score (p value)**	**ε**
Distance to mainland	-0.88 (<0.03)	0.20
Tidal range	0.4 (<0.06)	0.67
Cyclone frequency	-0.72 (<0.04)	0.45
Average exposed RWE	0.21 (<0.08)	0.27
% Vegetative cover	2.10 (<0.03)	3.89
Reef Area	-2.82 (<0.01)	1.31

Table 1 Summary diagnostics for the three highest performing autoregressive models for unvegetated cays, vegetated cays and low wooded islands (ε = standard error).

The highest performing models for unvegetated cays, vegetated cays and low wooded islands explained 89%, 73% and 79% of the variation in island characteristics respectively (Fig. 3).

Discussion

The overall efficacy of the models in explaining the observed variation in area and volume of the 103 analysis islands corroborated much of the basic theory on island dynamics (Smithers and Hopley, 2011). This includes the positive association of island development with tidal range, wave exposure and vegetative cover (Stoddart and Steers, 1977; Gourlay, 1988). In some cases the z-scores indicated a variable influence, for example, there is an inverse relationship between cyclone frequency and island volume for vegetated cays and low wooded islands, however, this was not the case for unvegetated cays, the areas of which seemed to vary in direct proportion to cyclone influence. The accretionary influence of cyclone and storm events has been observed through the reworking of rubble ramparts into stable landforms (Kench and Brander, 2006; Webb, 2006). The presence of vegetation appeared to reverse this relationship, which contrasts with the accepted role of vegetation as a sediment stabilizer (Heatwole, 2011), which has been linked statistically to decreased cay mobility (Aston, 1995). The area of the reef platform over which the island had developed had a positive relationship to island size for the unvegetated and vegetated cays, but a negative relationship for the low wooded islands. In the case of the unvegetated and vegetated cays, this positive relationship is likely underpinned by the delivery of greater volumes of sand from the productive forereef area, however, where low wooded islands have formed, the sand deposition may be less focused over the broader reef platforms or impeded by the windward development of a shingle ridge. This is reflected in the cross-shelf location of islands where a systematic difference can be seen in the height of reef surfaces due to hydro-isostatic shelf warping (Hopley, 2009), with low wooded islands forming on high reefs near the coast and sand and shingle cays on lower seaward reefs.

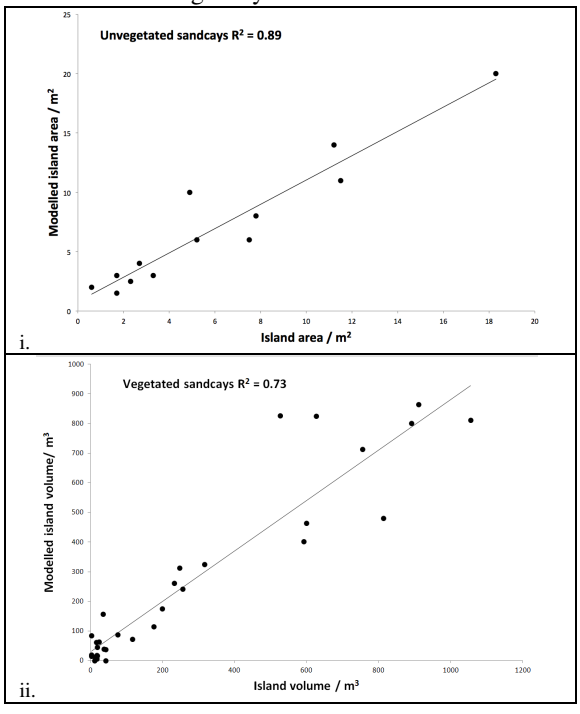

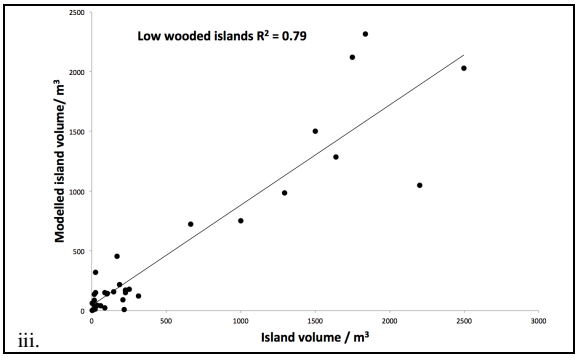

Figure 3: Modelled vs. actual island volumes and areas for i. unvegetated cays, ii. vegetated cays, and iii. low wooded islands.

It is worth noting that one of the key controls of island character, the amount of time since the island reached maturity, is not captured by this geospatial analysis. Nonetheless, the performance of these models indicates the value of these spatially referenced vector datasets for conducting regional scale analyses of island dynamics. This expands previous statistical investigations of island dimensions and regional patterns across latitudinal and cross-shelf gradients along the Great Barrier Reef (Hopley et al., 1989; Hopley et al., 2007) and studies of cay mobility (Aston, 1995) to define explicit links between regional environmental controls and island characteristics, such as area and volume. Although the models reported here sought to explain observed patterns, the empirical links defined could also be used in a predictive manner by substituting anticipated future values for local environmental controls. For example, the derived beta coefficient associated with a given variable such as cyclone frequency could be used to simulate the influence of cyclones on future island characteristics given parameterisation of anticipated future cyclone frequencies, (e.g. climate simulation models suggest a 56% increase in the number of storms with maximum winds greater than 30 m s^{-1}) (Walsh et al., 2004). Further developing the models in this way has the potential to go beyond an exploration of geographical patterns of contemporary landform characteristics to generate a coastal management tool for simulating future island accretionary and erosional dynamics, and consequent vulnerability to environmental change.

Acknowledgements

This analysis would not have been possible without the provision of the GBR features dataset from the *Great Barrier Reef Marine Park Authority*. Thanks to Adam Carrigan for essential pre-processing of the IBTRACS tropical cyclone data. Session Chairs are thanked for their help with the processing of this manuscript.

References

Anselin L, Bera A (1998) Spatial dependence in linear regression models with an introduction to spatial econometrics. In: Ullah A, Giles DE (eds) Handbook of applied economic statistics. Marcel Dekker Press, New York, pp 237–289

Aston JP (1995) The relative mobilities of coral cays on the Great Barrier Reef can be modeled. MSc Thesis, James Cook University, Townsville, p 267

Beaman R (2010) Project 3DGBR: A high resolution depth model for the Great Barrier Reef and Coral Sea. Marine and Tropical Sciences Research Facility (MTSRF) Project 2.5i.1a Final Report, Reef and Rainforest Research Centre, Cairns, Australia

Carrigan A, Puotinen M (2011) Assessing the potential for tropical cyclone induced sea surface cooling to reduce thermal stress on the world's coral reefs. GeoPhys Res Let 38:1-5

Fairbridge RW, Teichert C (1948) The Low Isles of the Great Barrier Reef: A new analysis. J Geog 111:67-88

Gourlay M (1988) Coral Cays: Products of wave action and geological processes in a biogenic environment. Proc 6th Int Coral Reef Sym 2:491-496

Heatwole, H (2011) Coral cays, vegetational succession. In: Hopley D (ed) Encyclopedia of Modern Coral Reefs: Structure, Form and Process. Springer, Berlin, pp 256-261

Hill N, Pepper A, Puotinen M, Hughes M, Leaper R, Edgar G Barrett, N (2010) Development of a quantitative relative wave exposure index for shallow reefs in temperate Australia. Mar Ecol Progr Ser 417:83-95

Hopley D, Parnell KE, Isdale PJ (1989) The Great Barrier Reef Marine Park: dimensions and regional patterns. Austral Geog Stud 27:47-66

Hopley D, Smithers SG, Parnell KE (2007) The Geomorphology of the Great Barrier Reef. Cambridge University Press, Cambridge, p 532

Hopley D (2009) Geomorphology of Coral Reefs with Special Reference to the Great Barrier Reef. In: Hutchings PA, Kingsford MJ, Hoegh-Guldberg O (eds) Coral Reefs of the World 2: The Great Barrier Reef Biology, Environment and Management. Springer, Berlin, pp 5-17

Kench PS, Brander RW, (2006) Response of reef island shorelines to seasonal climate oscillations: South Maalhosmadulu Atoll, Maldives. J Geophys Res 111:29-45

Landsea CW, Harper BA, Hoarau K, Knaff JA (2006) Can we detect trends in extreme tropical cyclones? Science 313:452-454

Longley PA, Goodchild MF, Maguire D, Rhind DW (2010) Geographic Information Systems and Science. Wiley, Chichester, p 515

Pepper A, Puotinen M (2009) GREMO: A GIS-based generic model for estimating relative wave exposure. Annual Proc Int Congress on Modelling and Simulation pp 1964-1970

Smithers S, Hopley, D (2011) Coral cay classification and evolution. In: Hopley, D. (ed) Encyclopedia of modern coral reefs: Structure, form and process. Springer, Berlin, pp 237-253

Stoddart DR, Steers JA (1977) The nature and origin of coral reef islands. In: Jones OA, Endean R (eds) Biology and Geology of Coral Reefs. Academic Press, New York, pp 59-105

Webb AP (2006) Coastal change analysis using multi-temporal image comparisons: Funafuti Atoll. SOPAC Technical Report 54

Walsh KJE, Nguyen KC, McGregor JL (2004) Fine-resolution regional climate model simulations of the impact of climate change on tropical cyclones near Australia. Climate Dynamics 22:47–56